The application of atomic layer deposition in the production of sorbents for $^{99}Mo/^{99m}Tc$ generator

Moret, J. L.T.M.; Alkemade, J.; Upcraft, T. M.; Oehlke, E.; Wolterbeek, H. T.; van Ommen, J. R.; Denkova, A. G.

DOI
10.1016/j.apradiso.2020.109266

Publication date
2020

Document Version
Final published version

Published in
Applied Radiation and Isotopes

Applied Radiation and Isotopes 164 (2020) 109266

Contents lists available at ScienceDirect

Applied Radiation and Isotopes

journal homepage: http://www.elsevier.com/locate/apradiso

The application of atomic layer deposition in the production of sorbents for ^{99}Mo/^{99m}Tc generator

J.L.T.M. Moret [a,b], J. Alkemade [a], T.M. Upcraft [a,b], E. Oehlke [a,c], H.T. Wolterbeek [a], J. R. van Ommen [b], A.G. Denkova [a,*]

[a] Applied Radiation and Isotopes, Radiation Science and Technology, Delft University of Technology, Delft, the Netherlands
[b] Process and Product Engineering, Chemical Engineering, Delft University of Technology, Delft, the Netherlands
[c] Department of Chemistry and Biotechnology, FH Aachen, University of Applied Sciences, Aachen, Germany

ARTICLE INFO

Keywords:
Sorbent materials
^{99}Mo/^{99}mTc

ABSTRACT

New production routes for ^{99}Mo are steadily gaining importance. However, the obtained specific activity is much lower than currently produced by the fission of U-235. To be able to supply hospitals with ^{99}Mo/^{99m}Tc generators with the desired activity, the adsorption capacity of the column material should be increased. In this paper we have investigated whether the gas phase coating technique Atomic Layer Deposition (ALD), which can deposit ultra-thin layers on high surface area materials, can be used to attain materials with high adsorption capacity for ^{99}Mo. For this purpose, ALD was applied on a silica-core sorbent material to coat it with a thin layer of alumina. This sorbent material shows to have a maximum adsorption capacity of 120 mg/g and has a^{99m}Tc elution efficiency of 55 ± 2% based on 3 executive elutions.

1. Introduction

^{99m}Tc is the most commonly used medical radionuclide accounting for around 40 million annual procedures worldwide (Association, 2014). This large demand is due to its favourable decay characteristics, i.e. emission of a low energetic gamma that can accurately be detected outside the body and a half-life of 6 h allowing for reasonable handling without exposing the patient to high radiation dose. In addition, its versatile chemistry allows Tc to be incorporated in diverse radiopharmaceuticals to study a variety of dysfunctions (Association, 2014; Molinski, 1982; Richards et al., 1982). Nevertheless, ^{99m}Tc would not have become such a widely used medical radionuclide if it was not for the development of a^{99}Mo/^{99m}Tc radionuclide generator (Richards et al., 1982). This radionuclide generator allows hospitals on demand supply of ^{99m}Tc. In the ^{99}Mo/^{99m}Tc radionuclide generator the parent isotope ^{99}Mo ($t_{1/2} = 66$ h) is immobilised on an alumina sorbent column, where it decays to ^{99m}Tc. The immobilisation of Mo occurs due to electrostatic interactions between the alumina sorbent and the molybdate ions. The produced ^{99m}Tc is eluted from the column using a saline solution whenever required (IAEA).

Currently, the majority of ^{99}Mo is produced via the fission of enriched uranium targets in nuclear research reactors, resulting in ^{99}Mo with a specific activity of ~10^4 Ci/g. The major drawbacks of uranium targets are that they produce large volumes of high activity (liquid) waste and that the production of ^{99}Mo depends on only six nuclear research reactors worldwide (Association, 2014; IAEA, 2013; Pillai et al., 2013). In 2008 unexpected shutdowns and maintenance led to worldwide shortages of ^{99}Mo (IAEA, 2013; Roobol et al., 2017). To overcome these major shortcomings, several alternative routes have been proposed and are currently being implemented. The most promising alternative routes at the moment are the following two reactions: the photon reaction with ^{100}Mo(γ,n)^{99}Mo and the neutron activation of ^{98}Mo, ^{98}Mo(n,γ)^{99}Mo (Association, 2014; IAEA, 2013). However, these alternative routes produce low specific activity ^{99}Mo ranging roughly from 10 to 100 Ci/g (IAEA, 2013). Simply increasing the sorbent mass of the generator is not an option, as this will require more shielding making transportation difficult and expensive, and will lead to larger elution volumes resulting in too low concentrations of ^{99m}Tc for medical applications (IAEA, 2013). Therefore, a more appropriate option is to develop sorbent materials having much higher adsorption capacity.

In previous research it was observed that when the surface area of the alumina sorbent material was increased the adsorption capacity for Mo increased (Denkova et al., 2013). However, there are no suitable alumina sorbents with very high surface areas available (i.e. surface area

* Corresponding author.
E-mail address: a.g.denkova@tudelft.nl (A.G. Denkova).

https://doi.org/10.1016/j.apradiso.2020.109266
Received 10 February 2020; Received in revised form 23 April 2020; Accepted 1 June 2020
Available online 11 June 2020

above 300 m^2/g). Therefore, our strategy is to take a different substrate with a very high surface area (e.g. silica), and to provide this surface with an ultrathin film of alumina via atomic layer deposition (ALD) allowing to alter the iso-electric point of the substrate and facilitate the adsorption of molybdenum ions. ALD is a versatile gas phase coating technique commonly used in the semi-conductor industry: many different substrates can be coated with a large number of different (functional) coatings (Miikkulainen et al., 2013; Puurunen, 2005). One ALD cycle consists of a precursor pulse and a co-reactant pulse separated by purge pulses. In ALD these reactions are self-limiting, meaning when the surface is saturated the reaction stops (Miikkulainen et al., 2013; Puurunen, 2003). This cyclic approach allows for nano-control of the material deposited. Furthermore, if ALD is carried out in a fluidised bed reactor (i.e. particles suspended in an upward gas flow) the process can be scaled up (King et al., 2007; Kunii and Levenspiel, 2013; Valdesueiro et al., 2015).

In this article we focus on the development of sorbent materials with increased adsorption capacity. We use ALD to introduce a thin layer of alumina on the surface of mesoporous silica, to alter its surface chemistry. After application of the alumina layer the adsorption capacity for Mo was determined and its potential to be used as sorbent material for a $^{99}Mo/^{99m}Tc$ radionuclide generator was assessed.

2. Materials and method

2.1. Chemicals

The SBA-15 substrate (highly structured SiO_2) was purchased from ACS materials (USA) and had a surface area of 570 m^2/g, a pore diameter of 7.5 nm and a particle size distribution of 1–4 μm. The substrate was dried overnight at 120 °C before use. Trimethylaluminum (TMA) was obtained from Akzo Nobel (Amersfoort, Netherlands) in a stainless steel bubbler. Purified water was obtained from an in-house Millipore System. The nitrogen was grade 5.0, supplied by a central gas line. MoO_3 99.9% was purchased from J.K. Baker. Radioactive Mo was obtained by irradiation MoO_3 for 1 h at a thermal neutron flux of $4.72*10^{16}$ n/m^2s, an epithermal neutron flux of $8.0 *10^{14}$ n/m^2 and a fast neutron flux of $3.48*10^{15}$ at the Reactor Institute Delft. NaOH, NaCl, HCl 30% and acid activated alumina (AA) were obtained from Sigma Aldrich and used without further purification.

2.2. Preparation of the sorbents

2.2.1. Set up

Atomic layer deposition (ALD) was performed in a custom-made fluidised bed reactor. The fluidised bed reactor consisted of a glass column with a diameter of 25 mm and a length of 500 mm mounted on a stainless steel wind box with a stainless steel porous plate. On top of the column also a porous plate and a metal vessel were connected. In this column the powdered substrate was suspended in an upward gas flow, allowing it to fluidize (i.e., it seems to behave like a liquid). The precursors were fed alternatingly into the reactor chamber using nitrogen as a carrier gas from the bottom of the reactor. The carrier gas flow was 0.5 l/min ($1.52 * 10^{-2}$ m/s). The fluidised bed was heated using an infra-red lamp. The whole system was controlled using a PC with a custom made Lab view program. The off gasses were washed with a series of wash bottles containing kydol oil and then a HEPA filter. The system was operated at atmospheric pressure at a temperature of 170 °C (van Ommen and Goulas, 2019).

2.2.2. Coating

The SBA-15 substrate was coated with alumina during 3–5 ALD cycles, each cycle consisting of 16 min–20 min–13 min–20 min TMA – purge – water – purge, respectively.

2.3. Adsorption experiments

The adsorption capacity of the sorbents was determined by soaking the sorbents in Mo containing solutions of starting concentrations ranging between 0.5 and 20 mg/mL for time periods of 1 min–120 min. The Mo solutions were prepared by dissolving MoO_3 in 1 M NaOH at a concentration of 25 Mo mg/mL. At the day of experiments, the stock solution was brought to pH 4 using 1 M HCl and then diluted to the desired concentration. For tracer experiments a small amount of ^{99}Mo (4MBq) was added to the dilutions. Before analysis the eluates were filtered using a 0.45 μm Whatman syringe filters to remove sorbent fines.

2.4. ^{99m}Tc elution efficiency

The ^{99m}Tc elution efficiency was determined by soaking the sorbents in a Mo solution containing ^{99}Mo. Therefore, MoO_3 was irradiated with neutrons at the Hoger Onderwijs Reactor (HOR) at TU Delft for 1 h at a thermal neutron flux of $4.72*10^{16}$ n/m^2s, epithermal thermal neutron flux of $4.5*10^{14}$ n/m^2s and a fast neutron flux of $3.5*10^{15}$ n/m^2s. After irradiation the Mo solution was prepared in the same way as the adsorption experiments. After soaking for 1.5 h the sorbent materials were washed three times with a physiological salt solution until pH of the liquid was 7. After washing the sorbent materials were set aside in a physiological salt solution to establish equilibrium between ^{99}Mo and ^{99m}Tc. After the ingrowth period the liquid was removed from the solid and filtered over a 0.45 μm filter before analysis.

2.5. Analysis

Elemental analysis of the sorbents was done by ICP-OES (Optima 4300, Perkin and Elmer). For this purpose, 50 mg of the sorbent material was dissolved in 6 mL Aqua Regia and 0.4 mL HF 40% under microwave assistance and then diluted to 50 mL with milliQ water in a volume flask. Furthermore, the coating was visualised by TEM and the change in surface area was determined by nitrogen adsorption BET theory (TriStar). The elemental content of the initial solution and of the eluents of adsorption were either determined by ICP-OES (non-radioactive samples and radioactive samples) or gamma spectroscopy (radioactive samples) (NaI crystal, Wallac^2 gamma counter, Perkin and Elmer). The adsorbed amount of Mo was determined by $q = \frac{m_{Mo,initial} - m_{Mo,\ eluate}}{m_{sorbent}}$.

3. Results and discussion

3.1. Characterisation of the sorbent material

The SBA-15 substrate material is coated with an alumina layer via ALD in a fluidised bed reactor using TMA and water. Samples are prepared applying 3 and 5 ALD cycles. The layer thickness of the deposited Al_2O_3 layer (d_{Al2O3}) is calculated according to Valdesueiro et al. (2015) based on the amount of Al deposited on the particles as determined by ICP-OES. Using this data, the growth per cycle (GPC) is derived (Table 1). The GPC is 0.32 ± 0.09 nm/cycle for deposition at 170 °C, which is rather high compared to literature values of 0.14 nm/cycle (Valdesueiro et al., 2015) or 0.1 nm/cycle (Kei et al., 2014). However, comparable GPC (0.2 nm/cycle) has been reported by Beetstra et al. (2009) under similar conditions. The dosing times calculated for coating the SBA-15 substrate are conservative, meaning that the substrate will be overexposed to TMA and water to make sure that the surface is saturated. Therefore, it is well possible that the high GPC is caused by overexposure of precursor in combination with a relatively short purging time. The atmospheric pressure in de reactor and the porous substrate can make it difficult to purge the system completely, which could contribute to the rather high GPC.

The surface area of the sorbent material decreases when applying the aluminium oxide coating (Table 1). This can be explained by the high

Table 1
Comparison of the physical characteristics of the currently used acid activated alumina (AA), the bare silica substrate (SBA-15) and the coated with Al_2O_3 silica sorbent (denoted as silica core xC, with x number of cycles). The film thickness (d_{Al2O3}) is calculated based on the ICP-OES results for the Al deposition on the particles.

Material	Al [w%]	dAl2O3 [nm]	GPC [nm/cycle]	Surface area [m2/g]	Pore diameter [nm]	Iso-electric point
AA (current sorbent standard)	54.9	N.A.	N.A.	170 ± 10	–	~6
SBA-15 (bare substrate)	–	–	–	592 ± 62	7.5	~2
Silica core 3C	12.9 ± 3.52	1.09 ± 0.36	0.37 ± 0.12	286 ± 36	6	n.d.
Silica core 5C	17.57 ± 0.04	1.64 ± 0.44	0.32 ± 0.09	247 ± 25	5.5	n.d.

porosity of SBA-15, which includes micro- and meso-pores (Fig. S2) that can get blocked when applying the aluminium oxide coating either due to their size or to the incomplete diffusion of TMA molecules all the way to the end of the pore. The initial pore size is around 6 nm while TMA molecule has a diameter of approximately 0.6 nm (Wiberg et al., 2001). It can therefore be expected that as the coating proceeds diffusion will become more difficult, and finally pore blockage will occur, leading to reduction of the surface area of the material. The micro-pores are expected to be almost entirely blocked when applying the coating, assuming a full layer is deposited. However, the surface area of the coated material is still 1.5 times higher than the acid activated alumina (AA) reference material.

Transmission electron microscopy (TEM) is used to visualise the coating. SBA-15 is described as a highly structured material with a honeycomb like structure (Denkova, 2009). This structure can be seen in Fig. 1 A. The Al_2O_3 layer as deposited is amorphous, which allows distinguishing between the substrate and the coating. Based on the TEM images a layer thickness of 2 nm is estimated for silica core 5C. This is in agreement with the calculated value using ICP-OES data and the estimated layer thickness based on the change in pore diameter. The layer thickness and the surface area for silica core 3C show large variation between batches. The differences probably originate from the fact that the first few cycles do not completely cover the surface of the support, due to for instance steric hindrance, creating a partial coating of Al_2O_3. (Puurunen, 2003). Additional cycles cover also the initially uncoated parts, resulting in a full layer of Al_2O_3. During the coating experiments it is observed that interactions between the glass column and the powder seems to change around the 4th cycle (i.e. less powder is sticking to the column wall) indicating a coating has been formed.

3.2. Stability assessment of the sorbent material

An important criterion for the sorbents is their stability during their use in a radionuclide generator and their behaviour during loading with ^{99}Mo. Therefore, a stability assessment of the SBA-15 core sorbent has been performed. In Fig. 2 the results of the stability assessment are shown. Almost the entire applied Al-layer has disappeared from the sorbent material at pH 1. This is expected considering the solubility of aluminium oxide at pH 1. Increasing the pH of the solution decreases the loss of Al from the sorbent material. At pH 3 only 0.19 ± 0.08 % of the Al deposited is lost, while at pH 4 and above no detectable amount of Al is present in the eluents. The detection limit for Al on ICP-OES is 0.02 mg/L (Group, 2007). Therefore, adsorption experiments of ^{99}Mo have been carried out at pH 4 or higher.

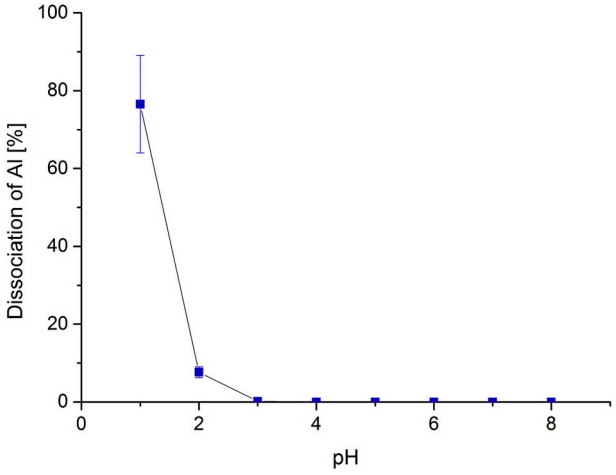

Fig. 2. Loss of Al from the sorbent material (silica core 5C) as function of pH. For each pH value a solution was prepared either with HCl or NaOH. The loss of Al is given as a percentage of the Al deposited on the substrate. Sorbent material with 5 cycles of ALD was used. The error bars correspond to the experimental uncertainty determined by n = 3. Above pH 4 and higher no Al could be measured in solution. The detection limit for ICP-OES is 0.02 mg/L.

3.3. pH influence on Mo adsorption

It is known that the pH of the solution has an influence on the adsorption capacity of the sorbent material due to the formation of different Mo species and their interaction with the sorbent (Denkova et al., 2013). Therefore, to determine the optimal pH for Mo adsorption Mo solutions of different pH vales have been prepared. The Mo adsorption of the silica core sorbent materials compared to the non-coated material at different pH values is shown in Fig. 3.

Clearly visible is that Mo adsorption decreases at higher pH values. The decrease in adsorption capacity can be explained by difference in speciation of Mo. At pH 4 and 5 there is a relatively large amount of Mo

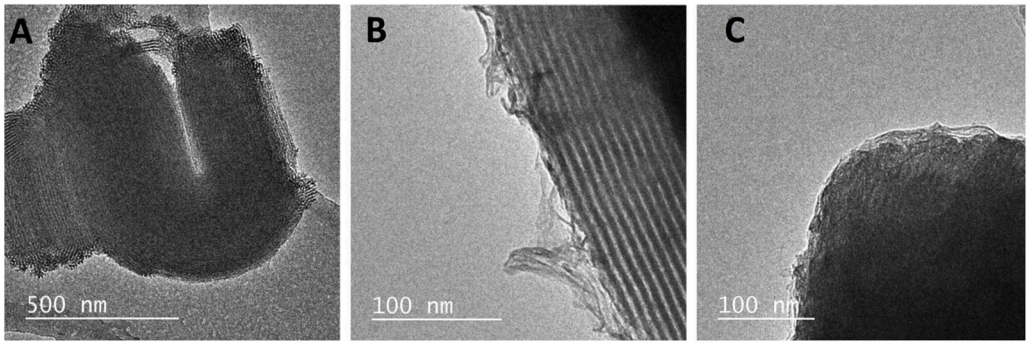

Fig. 1. TEM images of A) the bare substrate SBA-15, B) with 3 cycles and C) with 5 cycles of Al_2O_3.

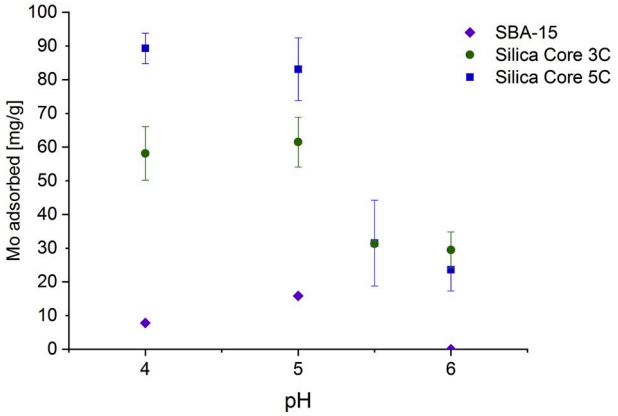

Fig. 3. Mo adsorption capacity of the sorbent material as function of pH compared to bare SBA-15 (590m^2/g) with a Mo concentration of 6 mg/mL and a sorbent concentration of 17 ± 3 mg/mL. A decrease in adsorption capacity is observed with increasing pH. Error bars are based on experimental uncertainties of n = 3. Purple diamonds are bare SBA-15, blue squares are the silica core 5C sorbent and the green rounds are the silica core 3C sorbent. (For interpretation of the references to colour in this figure legend, the reader is referred to the Web version of this article.)

species present that are highly negatively charged (e.g. $HMo_7O_{24}^{5-}$ and $Mo_7O_{24}^{6-}$), allowing for strong interaction with the positively charged surface. Increasing the pH causes the speciation to shift to less negatively charges species (Fig. 4). However, this speciation data is just an estimation of the speciation during adsorption which does not consider influences induced by the sorbent material (e.g. loss of Al from the sorbent material). Even though the used software to calculate the speciation, i.e. CHEAQs (Verweij, 2014–2017) (Chemical Equilibria in Aquatic solutions), has an extensive database, other species might exist. In addition, the iso-electric point of Al_2O_3 is 9 and as the pH increases, the sorbent material will become less positively charged weakening the interaction with negatively charged species. However, the coated material having 5 cycles shows a significant increase in Mo adsorption capacity compared to bare SBA-15 and the sorbent material made with 3 cycles of ALD. This trend can be explained by the amount of Al present on the sorbent material. Bare SBA-15 (No Al) has an iso-electric point of 2, meaning that at the pH tested the material is negatively charged, limiting its interaction with the negatively charged Mo species. The material coated with 3 ALD cycles has an incomplete coating, as explained above, and so will have spots where reduced adsorption is occurring due to bare SBA-15 being exposed. Because of the decrease in Mo adsorption at higher pH values, further experiments have been carried out at pH 4, which is in agreement with the loading conditions currently used in ^{99}Mo/^{99m}Tc generators. (IAEA).

3.4. Kinetic behaviour of the sorbent material

The adsorption kinetics of the ALD prepared sorbent materials is determined by submersing the sorbent materials in a Mo solution for different time periods. After filtration the Mo and Al concentration in the eluate is determined. The amount of Mo adsorbed is calculated from the difference in Mo concentrations before and after contact with the sorbent material. Acid activated alumina (AA) is always used as control sorbent. The adsorption results are given in Fig. 5.

The experimental data is analysed using a kinetic model: a pseudo – second order fit (Equation (1)). In this model q_t is the adsorption capacity at time t, q_e is the adsorption capacity at equilibrium and k_2 is the pseudo second order rate constant. The pseudo – second order model is generally used to describe molybdenum adsorption and is therefore used to be able to compare our results to other sorbent materials reported in literature. The obtained fit parameters are given in Table 2.

$$q_t = \frac{k_2 q_e^2 * t}{1 + k_2 q_e * t} \quad [1]$$

As already can be seen in Fig. 5 the data points are rather scattered, especially for the silica core sorbent material. This scattered data is reflected in the low values for the correlation coefficient (R^2) (Table 2) of the fit. During the production of the silica core sorbent material agglomerates are formed. Where the particles permanently attached to each other within these agglomerates no coating will take place at these touching points. This causes the individual particles to be heterogeneously coated. When suspending the silica core sorbent material in solution, it is possible that the agglomerates break, exposing uncoated sorbent material. Also there could be a slight difference in speciation of the molybdate ions between experiments, due to batch differences. Unfortunately, due to the low correlation coefficients the obtained values cannot be compared to the literature. However, it is clear that the Mo adsorption is very fast and equilibrium for both the AA and the silica core sorbent are reached within 2 h. Furthermore, the adsorption rate constant for the silica core sorbent is an order of magnitude smaller compared to the AA sorbent. Considering the high porosity of this

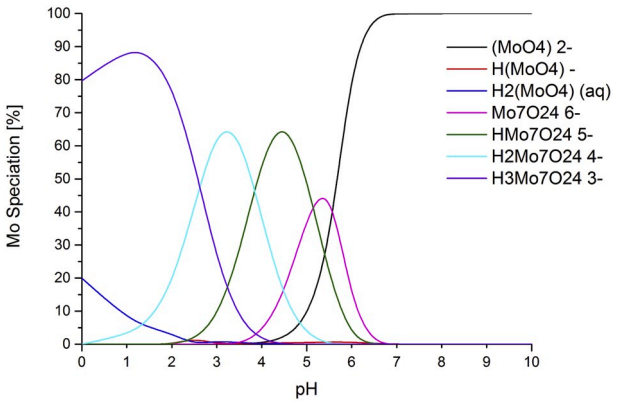

Fig. 4. The Mo speciation in solution at equilibrium for different pH values. The speciation is calculated using CHEAQS for a fixed concentration (6 mg/mL Mo) at 20 °C and without any sorbent material. Black line: $(MoO_4)^{2-}$, red line: $H(MoO_4)^-$, blue line: $H_2(MoO_4)_{(aq)}$, pink line: $Mo_7O_{24}^{6-}$, green line: $HMo_7O_{24}^{5-}$, cyan line: $H_2Mo_7O_{24}^{4-}$ and purple line: $H_3Mo_7O_{24}^{3-}$. (For interpretation of the references to colour in this figure legend, the reader is referred to the Web version of this article.)

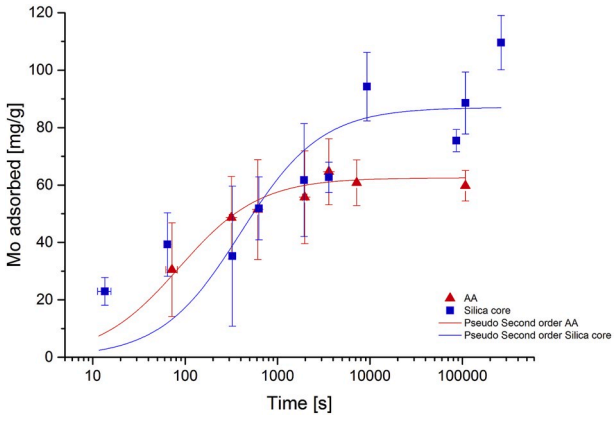

Fig. 5. Mo adsorbed concentration as function of contact time. Initial Mo concentration is 9.1 ± 0.7 mg/mL, initial pH 4, sorbent concentration is 17 ± 3 mg/mL and temperature is 20 °C. Blue squares represent silica core 5C and red triangles denote AA. The lines represent the pseudo second order fit of the data. Error bars are based on experimental uncertainties of n = 4. (For interpretation of the references to colour in this figure legend, the reader is referred to the Web version of this article.)

Table 2
Pseudo second order parameters obtained for the adsorption of Mo on the silica core 5C sorbent compared to AA using a starting concentration of 9 mg/mL of Mo at pH 4 and T = 20 °C, with a sorbent concentration of 17 ± 3 mg/mL. The data is nonlinearly fitted according to equation (1).

Sorbent	k_2 [g/mg s]	q_e [mg/g]	R^2
AA	$(1.85 \pm 0.53)*10^{-4}$	62.53 ± 2.82	0.60
Silica core 5C	$(2.86 \pm 0.96)*10^{-5}$	87.04 ± 5.59	0.50

material it is possible that there are diffusion limitations which lowers the adsorption rate, as to fully utilise all available surface area the molybdate ions have to diffuse into the 6 ± 0.5 nm pores of the silica core sorbent material.

3.5. Stability of the coating during loading

The Al concentration measured in the eluate is a measure for the stability of the sorbent material during loading of Mo. Using this concentration, the Al loss percentage was determined. The Al loss of AA is negligible, while for the silica core sorbent this Al loss percentage is 4.27 ± 3.07 % of the amount of Al originally present on the sorbent material. It is assumed that this Al loss is caused by the interaction of the molybdate ions with the amorphous alumina surface. Crystalline alumina is more stable than amorphous alumina (Miikkulainen et al., 2013). Therefore, part of the silica core sorbent material was annealed at 800–1100 °C, to transform the amorphous alumina layer to a more crystalline structure. XRD indicates that a crystalline structure was formed at 900 °C (see supplemental information S3). However, annealing of the silica core sorbent caused the pore structure of SBA-15 to collapse, reducing the surface area significantly (Table 3). That in return reduces the adsorption capacity enormously (Fig. 6). At 800 °C the surface area appeared unaffected but nevertheless the adsorption capacity decreased indicating that other processes play a role. It is possible that due to annealing the hydroxyl groups on the surface of the Al_2O_3 coating got removed or replaced by hydrogen groups, reducing the amount of active adsorption sites. The deposited Al_2O_3 coating is –OH terminated, because of the water pulse in the ALD process.

The instability of the alumina coating can also be attributed to the Cl^- concentration of the solution. When preparing the Mo solutions prior to use, the pH of part of the stock solution is lowered by adding HCl. As different Mo concentrations were prepared, also different HCl concentrations were needed. In order to determine the influence of the Cl^- ions Mo solutions of same concentration (5 mg/mL and 24 mg/mL at pH 5) are prepared with a different Cl^- concentration. Either the desired Mo concentration was prepared in 1 M NaOH and then brought to pH 5 with HCl or first a stock solution was made, of which a part was brought to pH 5 and then diluted to the desired Mo concentration. Mo adsorption results and Al loss are given in Table 4. The results actually indicate that a higher Cl^- concentration seems to stabilise the Al_2O_3 coating. However, this also decreases the adsorption capacity of the silica core sorbent material. This is observed for both Mo concentrations. It is assumed that the Cl^- is occupying active sites where otherwise molybdenum species would adsorb.

Table 3
Surface area of the silica core sorbent after annealing at several temperatures in air.

Annealing temperature [°C]	Surface area [m^2/g]
As deposited	276
800	265
900	175
1000	5.2*
1100	4.9*
800 (argon atmosphere)	266

*Some care must be taken with these numbers, as they are around the detection limit of the machine.

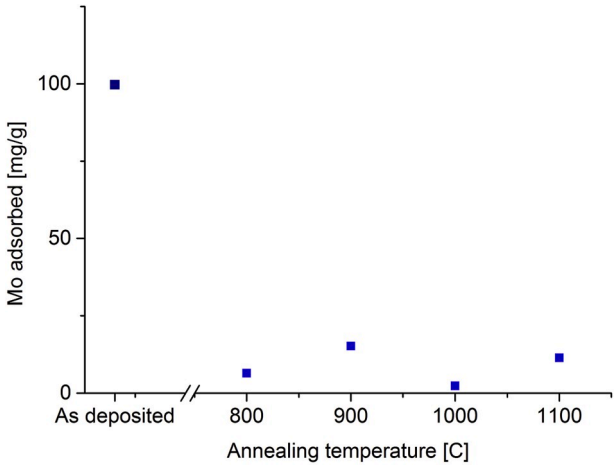

Fig. 6. Mo adsorption capacity as function of the annealing temperature for the silica core sorbent material. The temperature of the reaction chamber at which the Al_2O_3 layer was deposited was 230 °C. Mo concentration was 6 mg/mL and the sorbent concentration was 17 mg/mL.

Table 4
The effect of the Cl^- concentration on the Al loss of the silica core sorbent material and its Mo adsorption capacity for both a Mo start concentration of 5 mg/mL and 24 mg/mL. The initial pH of the solutions was pH 5. Direct preparation means that the desired Mo concentration was prepared in 1 M NaOH and then brought to pH 5 with HCl, diluted preparation means first a stock solution was made, of which a part was brought to pH 5 and then diluted to the desired Mo concentration.

	Mo start concentration 5 mg/mL		Mo start concentration 24 mg/mL	
	Direct preparation	Diluted preparation	Direct preparation	Diluted preparation
HCl concentration [M]	1.06	0.189	2.08	0.667
Al loss [mg/g sorbent	3.6	10.5	10.6	146
Mo adsorption [mg Mo/g sorbent	70.5	90.5	121	171

Isotherm behaviour of the sorbent material – Standard method.

To determine the maximum adsorption capacity of the sorbent materials, an adsorption isotherm is made. To this extent the sorbent materials is contacted with Mo solutions of different concentrations for 60 min to reach different equilibrium concentrations (Fig. 7). The experimental data is then analysed using three isotherm models: the Langmuir model (Equation (2)), the extended Langmuir model (Equation (3)) and the Freundlich model (Equation (4)), to describe the adsorption process. In these models q_e is the adsorption capacity at equilibrium, $q_{e,max}$ the maximum adsorption capacity, C_e the concentration of Mo at equilibrium, K_L, K_{eL} and K_F are the Langmuir constant, the extended Langmuir constant and the Freundlich constant, respectively. n_F and n_{eL} are model parameters. The Langmuir model is used to describe the adsorption of monolayers on the sorbent surface. It assumes that after adsorption the molecules stay at their adsorption site. The extended Langmuir model takes multilayer adsorption into account. The Freundlich model is an empiric model that can describe the adsorption on a heterogeneous surface for both monolayer and multilayer systems. The fitted results are given in Table 5.

$$q_e = \frac{q_{e,max} K_L C_e}{1 + K_L C_e} \quad [2]$$

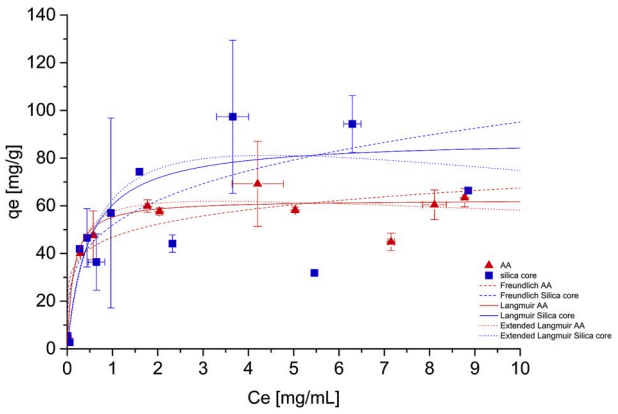

Fig. 7. Mo adsorption capacity as function of Mo equilibrium concentration. Red triangle is AA and blue square is Silica core. Dotted line corresponds to the extended Langmuir model, dashed line to the Langmuir model and full line to the Freundlich model. Sorbent concentration is 17 mg/mL, initial pH is 4 and T is 20 °C. Error bars are based on the experimental uncertainty of n = 3. (For interpretation of the references to colour in this figure legend, the reader is referred to the Web version of this article.)

Table 5
Adsorption parameters obtained from the isotherm fits for Mo ions at initial pH 4 for Langmuir, and Freundlich model.

	Langmuir			Freundlich		
Sorbent	K_L [mL/mg]	$q_{m,L}$ [mg/g]	R^2	K_F [mL/g]	$1/n_F$ [−]	R^2
AA	7.52 ± 1.54	62.55 ± 1.67	0.812	46.81 ± 1.8	0.16 ± 0.02	0.634
Silica core 5C	2.18 ± 0.61	88.09 ± 6.66	0.582	51.87 ± 3.65	0.26 ± 0.04	0.472

$$q_e = \frac{q_{e,max} K_{eL} C_e}{1 + K_{eL} C_e} \exp\left(\frac{n_{eL} C_e}{C_{max}}\right) \quad [3]$$

$$q_e = K_F C_e^{\frac{1}{n_F}} \quad [4]$$

From the fitted models, the Langmuir model fit the data best (R^2 = 0.81 and R^2 = 0.58 for AA and Silica core sorbent, respectively). Even though, the extended Langmuir model has comparable correlation coefficients (S4), using a more complex model has no added value when it does not give a significant improvement. However, the Langmuir model does have its shortcomings. It assumes no interaction between the adsorbent and the sorbent material and no movement of adsorbent over the surface (Toor and Jin, 2012). Judging by the Al loss from the silica core sorbent material during loading, there is some kind of interaction between the adsorbent and the sorbent. The stability of the formed Mo-sorbent complex is given by the Langmuir constant. This indicates that the adsorption on the silica core sorbent is slightly less stable compared to that of AA (by a factor 3.4, Table 5). However, the obtained Langmuir constant of AA is an order of magnitude lower then reported by Denkova et al. (2013). Partially, the difference can be attributed to the different adsorption pH values used in this paper. Furthermore, temperature and additional elements like Na^+ and Cl^- in solution can influence the Mo-sorbent complex stability. The obtained from the fit maximum adsorption capacities are in accordance with the plotted data.

Even though the Freundlich model does not fit the data as well as the Langmuir models, it still gives some information about the adsorption process. An $n_F > 1$ indicates a strong affinity between the adsorbent and the sorbent, which is in agreement with the rapid adsorption process.

3.6. Isotherm behaviour of the sorbent material – compartment method

The ionic strength of the Mo solutions partly depends on the Mo concentration of the different concentrations used to determine the isotherm. Therefore, to take this effect into account, the Mo starting concentration was kept constant and the ratio between the solid sorbent and the Mo-liquid was varied. By doing so the adsorption of Mo to the sorbent material can be represented by a two-compartment closed system. Assuming that the interaction of Mo with the container can be neglected due to inert container material, a simple model as shown in Fig. 8 can be derived.

The Mo concentration in the solvent can be described by equation (5) and the adsorbed Mo onto the sorbent material by equation (6). For derivation of these equations see supporting information S1. These equations assume a linear correlation between the adsorbed Mo amount and the sorbent to solvent ratio. However, as see in Fig. 9 the data shows somewhat exponential correlation and would be more appropriate using a model such as shown by equation (7). The determined q_m for AA is 81 mg/g and for silica core 5c is 127 mg/g.

$$C_V = \frac{C_0 + \frac{M}{V} q_0}{k_1 + k_2} k_2 + \left(\frac{C_0 + \frac{M}{V} q_0}{k_1 + k_2} k_1 - \frac{M}{V} q_0 \right) e^{-(k_1 + k_2)t} \quad [5]$$

$$q_m = \frac{\frac{V}{M} C_0 + q_0}{k_1 + k_2} k_1 - \left(\frac{\frac{V}{M} C_0 + q_0}{k_1 + k_2} k_1 - q_0 \right) e^{-(k_1 + k_2)t} \quad [6]$$

$$q_e = \frac{q_m * \frac{V}{M}}{K + \frac{V}{M}} \quad [7]$$

When the system is at equilibrium the mass flow rates will be equal in magnitude: $F_1 \underline{\text{def}} F_2$. From this equilibrium definition the equation describing the adsorbed amount as function of the solvent over sorbent ratio can be derived. Logic dictates that when V/M goes to infinity, q_m reaches its maximum and C_V assumes C_0. At large V/M ratios the mass of the sorbent becomes insignificant compared to the amount of solvent in the system and therefore the amount of adsorbed Mo will have no impact on the concentration in solution. The sorbent has reached it maximum adsorption capacity. This effect is already visible in the data presented in Fig. 9.

During analysis of the eluents it is noted that the concentrations in the eluents after adsorption still differ, meaning that the ionic strength of the solutions is still different. Therefore, for the attempt to keep the ionic strength of the solution constant, the compartment method has no

Table 6
Batch extraction properties of the different sorbents. The sorbent and Mo concentration during loading were 19 ± 3 mg/mL and 6.7 mg /mL respectively. The AA sorbent and the silica core 5C sorbent were loaded with *43.8* ± 20 mg *Mo/g sorbent and 19.8* ± *4.2* mg *Mo/g/sorbent respectively. Extraction* properties are based on the experimental average of n = 3. Loading capacity is based on n = 2. Extraction 1 and 2 are after 1 day of ingrowth. Between extraction 2 and 3 there is a period of 3 days ingrowth.

	Extraction 1			Extraction 2			Extraction 3		
Sorbent	^{99m}Tc [%]	^{99}Mo/^{99m}Tc [%]	Al [ppm]	^{99m}Tc [%]	^{99}Mo/^{99}mTc [%]	Al [ppm]	^{99m}Tc [%]	^{99}Mo/^{99m}Tc [%]	Al [ppm]
AA	*66.4 ± 1.9*	*2.08 ± 0.02*	*28.3 ± 0.9*	*56.8 ± 1.7*	*0.36 ± 0.01*	*4.63 ± 0.16*	*68.2 ± 4.3*	*0.18 ± 0.0*	*2.91 ± 0.11*
Silica core 5C	*54.9 ± 0.9*	*1.01 ± 0.09*	*1.32 ± 0.36*	*50.7 ± 0.5*	*0.34 ± 0.01*	*0.60 ± 0.01*	*59.5 ± 1.9*	*0.31 ± 0.02*	*0.54 ± 0.03*

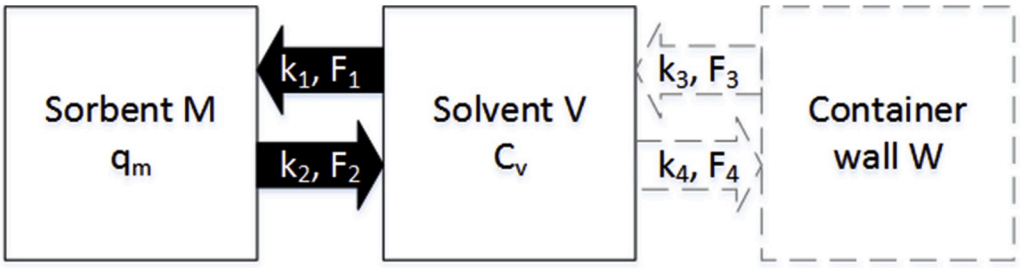

Fig. 8. Schematic representation of the compartments in the sorbent-solvent system during adsorption. The container wall is assumed not to participate in the adsorption of Mo. *k1* and k_2 are the rate constants for adsorption and desorption respectively and F_1 and F_2 are the corresponding mass flow rates.

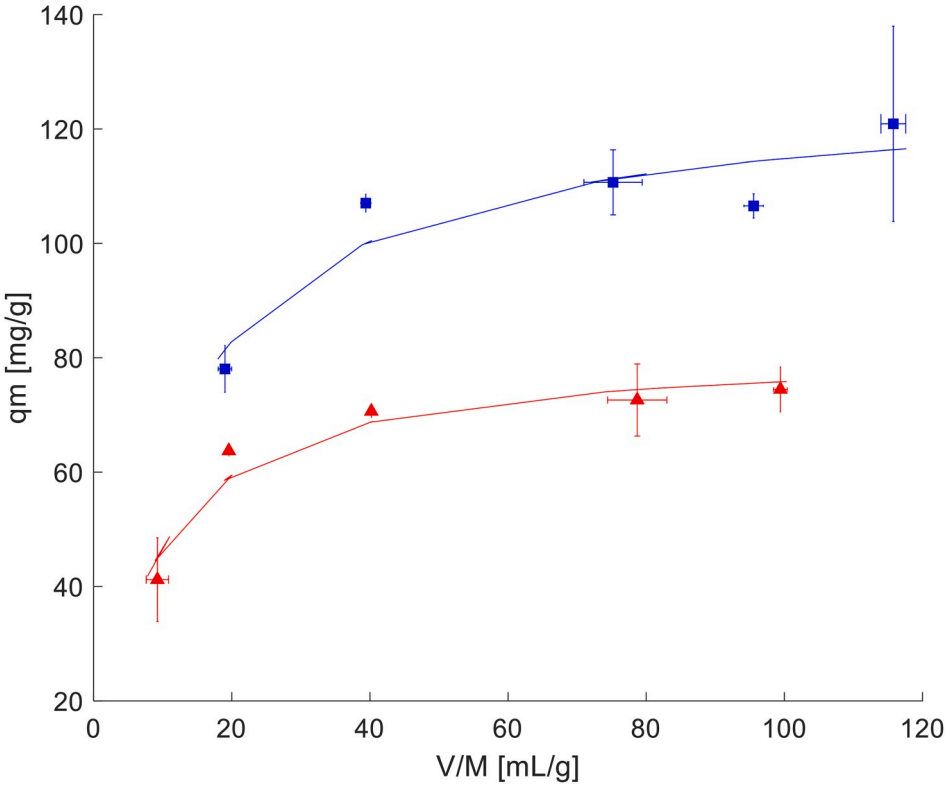

Fig. 9. Adsorption isotherm of Mo ions, using the compartment method, at pH 4. Blue squares represent the silica core 5c sorbent and the red triangles represent AA. The lines represent the fit using equation (6). Error bars are based on n = 3. (For interpretation of the references to colour in this figure legend, the reader is referred to the Web version of this article.)

added value over the standard method. Also, the adsorption capacities determined using this method do not significantly differ from the adsorption capacities determined using the standard method. However, the use of the compartment method seems to be a more reliable method due to smaller deviations in the results. This could be because at the start of the experiment the speciation for all the samples is the same, as the same Mo-solution is used. Using the standard method, the starting concentrations of Mo in solution differs and hence its speciation.

3.7. Pilot generator

For the sorbents to be a viable alternative for the currently used sorbent not only the adsorption capacity for Mo should be high enough, also ^{99m}Tc should be efficiently eluted from the radionuclide generator. Therefore, the sorbents are loaded with neutron activated ^{99}Mo and then eluted with a physiological salt solution. After loading the sorbents are washed with a physiological salt solution until pH was 7. Then the sorbents are left to reach equilibrium. The ingrowth period until elution 1 and 2 is 1 day, and the ingrowth period until elution 3 is 3 days.

With a loading capacity of 43.8 ± 20 mg/g, the loading of the AA sorbent material is as expected and comparable to previous results. On the other hand, the loading capacity of the silica core sorbent material is only 19.8 ± 4.2 mg/g, which is rather low and different from previously obtained results. Due to circumstances, between the production of the silica core 5C sorbent material and the use of this material as a sorbent at least a year has passed. Silica is known to be hygroscopic, which could affect the loading capacity. To minimise this effect the silica core sorbent material is stored under vacuum until use. Before these pilot generator experiments the silica core 5C sorbent material has been dried overnight, but it is possible that still water was present. In comparison, the undried silica core sorbent material has an adsorption capacity of 10.2 ± 1.6 mg/g.

It has to be noted that the extraction experiments were carried out in batch mode, while radionuclide generators are operated in column mode. Unfortunately, batch mode makes it more difficult to remove residual Mo from the sorbent material, indicated by the reduction of Mo loss with each consecutive extraction. In batch mode the sorbent material is fully loaded, while in column mode this is usually not the case.

Therefore, in column mode any desorbed Mo can re-adsorb somewhere further on the column, while this is impossible in batch mode.

The set limits for Mo-breakthrough and Al concentration in the eluate are 0.15 μCi Mo per 1 mCi ^{99m}Tc (0.15%) and 10 ppm Al (Convention, 2005; Tkac and Paulenova, 2008). This means that for both the AA sorbent and the silica core sorbent the Mo-concentrations in the eluate exceed the set limits. The relative high Mo breakthrough could be due to the high loading of the sorbent material. If a Mo-atom desorbs it is difficult to reabsorb when the sorbent material is close to its maximum loading capacity. Secondly, these experiments are carried out in batch mode. Together, this could cause the elevated breakthrough.

The Al breakthrough for the silica sorbent material is structurally lower compared to the AA sorbent material. This is surprising, as during loading of the sorbent materials the silica core sorbent material had a higher loss of Al. It is possible that the Cl^- ions in the salt solution stabilises the alumina layer on the silica core sorbent material. The Al concentration of the first elution of the AA sorbent material is comparable to the concentrations reported by Denkova et al. (2013).

The extraction efficiency of the silica core sorbent material (~55%) is structurally lower compared to the AA sorbent material (~65%) Table 6. During the experiments it proved to be more difficult to separate the liquid phase from the solid phase for the silica core sorbent compared to the AA sorbent due to the fine structure of the silica sorbent material.

3.8. Overall discussion

The aim of this paper was to investigate novel sorbent materials for a ^{99}Mo/^{99m}Tc radionuclide generator. A simple and straight forward calculation shows that an adsorption capacity of at least 166 mg Mo/g sorbent is required when a specific activity of 222 GBq/g is used for a 2 g column, taking into account that the European market wants to be supplied with 74 GBq ^{99}Mo generators. This calculation is based on 100 % loading which will not be applied due to high Mo breakthrough. Loadings of 30% are more realistic to reduce the chance of Mo breakthrough, and therefore an adsorption capacity of at least 555 mg Mo/g sorbent would be required. This adsorption capacity means that a 27 fold increase compared to the currently used aluminium oxide sorbent material needs to be achieved (Molinski, 1982). Attempts have been made to find sorbents with a higher adsorption capacity (Aulmann et al., 1983; Chakravarty et al., 2012; El-Absy et al., 2014), only none has succeeded in reaching the desired capacity of 555 mg Mo/g sorbent, however values up to 200 mg Mo/g sorbent were reported (Chakravarty et al., 2012). The adsorption capacity of 555 mg Mo/g sorbent can also not be reached using the silica core sorbent. The most likely cause for this is the reduction in surface area due to the applied coating. However, compared to the bare material, the adsorption capacity is significantly increased (by a factor 9), showing that the iso-electric point of the material can be properly changed. Also, the adsorption capacity of the silica core material is two-fold increase compared to the currently used AA.

4. Conclusions

ALD is a versatile coating technique that can be used to modify the surface properties of high-surface-area materials. The silica core sorbent material obtained using ALD can be used to adsorb Mo. The adsorption capacity obtained for this material is twice higher than that of the currently used AA. However, the adsorption capacity should be further increased to make it deployable in radionuclide generators using low specific activity ^{99}Mo. As the speciation of molybdenum seems to interfere with the adsorption capacity, using a compartment method over the standard method to determine isotherms increases the reliability of the obtained results. ^{99m}Tc can be eluted from the particles with an efficiency of 59.5 ± 1.9 %, which should increase. Furthermore, the Mo breakthrough should be reduced.

Declaration of competing interest

The authors declare that they have no known competing financial interests or personal relationships that could have appeared to influence the work reported in this paper.

CRediT authorship contribution statement

J.L.T.M. Moret: Supervision, Formal analysis, Writing - original draft. **J. Alkemade:** Formal analysis, Investigation. **T.M. Upcraft:** Formal analysis, Investigation. **E. Oehlke:** Supervision. **H.T. Wolterbeek:** Writing - review & editing. **J.R. van Ommen:** Writing - review & editing, Supervision. **A.G. Denkova:** Writing - review & editing, Supervision.

Acknowledgements

This research is part of a project funded by the NWO under project number 13306 and IDB-Holland B.V. Willy Rook is thanked for her help with the nitrogen adsorption. Kees Goubitz is thanked for his help with the XRD analysis. Aris Goulas is thanked for assistance in sorbent production.

Appendix A. Supplementary data

Supplementary data to this article can be found online at https://doi.org/10.1016/j.apradiso.2020.109266.

References

Association, W.N., 2014. Radioisotopes in Medicine. Acced on. http://www.world-nuclear.org/info/non-power-nuclear-applications/radioisotopes/radioisotopes-in-medicine/. (Accessed 24 February 2015).

Aulmann, M.A., Siri, G.J., Blanco, M.N., Caceres, C.V., Thomas, H.J., 1983. Molybdenum adsorption isotherms on y-alumina. Appl. Catal. 7, 139–149.

Beetstra, R., Lafont, U., Nijenhuis, J., Kelder, E.M., Van Ommen, J.R., 2009. Atmospheric pressure process for coating particles using atomic layer deposition. Chem. Vap. Depos. 15, 227–233. https://doi.org/10.1002/cvde.200906775.

Chakravarty, R., Ram, R., Dash, A., Pillai, M.R., 2012. Preparation of clinical-scale ^{99}Mo/^{99m}Tc column generator using neutron activated low specific activity ^{99}Mo and nanocrystalline gamma-Al_2O_3 as column matrix. Nucl. Med. Biol. 39, 916–922. https://doi.org/10.1016/j.nucmedbio.2012.03.010.

Convention, U.S.P., 2005. Official Monograph USP 28, Sodium Pertechnetate 99mTc Injection, p. 1861.

Denkova, A.G., 2009. Synthesis of SBA-15, applying the knowledge, Fundamentals of triblock copolymer self-assambly into solutions, and its realtion to nano-templating.

Denkova, A.G., Terpstra, B.E., Steinbach, O.M., Dam, J.t., Wolterbeek, H.T., 2013. Adsorption of molybdenum on mesoporous aluminum oxides for potential application in nuclear medicine. Separ. Sci. Technol. 48, 1331–1338. https://doi.org/10.1080/01496395.2012.736443.

El-Absy, M.A., El-Amir, M.A., Fasih, T.W., Ramadan, H.E., El-Shahat, M.F., 2014. Preparation of ^{99}Mo/^{99m}Tc generator based on alumina ^{99}Mo-molybdate (VI) gel. J. Radioanal. Nucl. Chem. 299, 1859–1864. https://doi.org/10.1007/s10967-014-2930-7.

Group, E.A., 2007. ICP-OES and ICP-MS Detection Limit Guidance.

IAEA, 2013. Non-HEU Production Technologies for Molybdenum-99 and Technetium-99m, NF-T-5, 4 ed. IAEA, Vienna, Austria.

Kei, C.C., Yu, Y.S., Racek, J., Vokoun, D., Šittner, P., 2014. Atomic layer-deposited Al2O3 coatings on NiTi alloy. J. Mater. Eng. Perform. https://doi.org/10.1007/s11665-014-0956-1.

King, D.M., Spencer Ii, J.A., Liang, X., Hakim, L.F., Weimer, A.W., 2007. Atomic layer deposition on particles using a fluidized bed reactor with in situ mass spectrometry. Surf. Coating. Technol. 201, 9163–9171. https://doi.org/10.1016/j.surfcoat.2007.05.002.

Kunii, D., Levenspiel, O., 2013. Fluidization Engineering. Elsevier.

Miikkulainen, V., Leskelä, M., Ritala, M., Puurunen, R.L., 2013. Crystallinity of inorganic films grown by atomic layer deposition: overview and general trends. Appl. Phys. Rev. 113.

Molinski, V.J., 1982. A review of ^{99m}Tc generator technology. Int. J. Appl. Radiat. Isot. 33, 811–819. https://doi.org/10.1016/0020-708X(82)90122-3.

Pillai, M.R., Dash, A., Knapp Jr., F.F., 2013. Sustained availability of ^{99m}Tc: possible paths forward. J. Nucl. Med. : Off. Publ. Soc. Nucl. Med. 54, 313–323. https://doi.org/10.2967/jnumed.112.110338.

Puurunen, R.L., 2003. Growth per cycle in atomic layer deposition: a theoretical Model. Chem. Vap. Depos. 9, 249–258. https://doi.org/10.1002/cvde.200306265.

Puurunen, R.L., 2005. Surface chemistry of atomic layer deposition: a case study for the trimethylaluminum/water process. J. Appl. Phys. 97, 121301. https://doi.org/10.1063/1.1940727.

Richards, P., Tucker, W.D., Srivastava, S.C., 1982. Technetium-99m: an historical perspective. Int. J. Appl. Radiat. Isot. 33, 793–799. https://doi.org/10.1016/0020-708X(82)90120-X.

Roobol, L.P., Reijden, A.v.d., de Waard - Schaik, I.R., Bijwaard, H., 2017. Productie en gebruik van medische radio-isotopen in Nederland. Huidige situatie en toekomstverkenning. In: RIVM), R.v.V.e.M. (Ed.), Bilthoven. https://doi.org/10.21945/RIVM-2017-0063.

Tkac, P., Paulenova, A., 2008. Speciation of molybdenum (VI) in aqueous and organic phases of selected extraction systems. Separ. Sci. Technol. 43, 2641–2657.

Toor, M., Jin, B., 2012. Adsorption characteristics, isotherm, kinetics, and diffusion of modified natural bentonite for removing diazo dye. Chem. Eng. J. 187, 79–88. https://doi.org/10.1016/j.cej.2012.01.089.

Valdesueiro, D., Meesters, G., Kreutzer, M., van Ommen, J.R., 2015. Gas-phase deposition of ultrathin aluminium oxide films on nanoparticles at ambient conditions. Materials 8, 1249–1263.

van Ommen, J.R., Goulas, A., 2019. Atomic layer deposition on particulate materials. Mater. Today Chem. 14.

Verweij, W., 2014-2017. Calculating CHemical Equilibria in AQuatic Systems, 3 ed. CHEAQS Next, p. P2017.

Wiberg, E., Wiberg, N., Holleman, A.F., 2001. Inorganic Chemistry. Academic Press ; De Gruyter, San Diego; Berlin; New York.